Characteristics of the terahertz radiation from single crystals of *N*-substituted 2-methyl-4-nitroaniline

2001 J. Phys.: Condens. Matter 13 L529

(http://iopscience.iop.org/0953-8984/13/23/101)

INSTITUTE OF PHYSICS PUBLISHING JOURNAL OF PHYSICS: CONDENSED MATTER

J. Phys.: Condens. Matter **13** (2001) L529–L537 www.iop.org/Journals/cm PII: S0953-8984(01)24148-4

LETTER TO THE EDITOR

Characteristics of the terahertz radiation from single crystals of *N*-substituted 2-methyl-4-nitroaniline

Hideki Hashimoto[1,4], Hironori Takahashi[2], Takashi Yamada[1], Kazuyoshi Kuroyanagi[2] and Takayoshi Kobayashi[3]

[1] Department of Materials Science and Chemical Engineering, Faculty of Engineering, Shizuoka University, 5-1 Johoku 3-Chome, Hamamatsu 432-8561, Japan
[2] Central Research Laboratory, Hamamatsu Photonics K. K., 5000 Hirakuchi, Hamakita 434-8601, Japan
[3] Department of Physics, Graduate School of Science, University of Tokyo, 7-3-1 Hongo, Bunkyo-ku, Tokyo 113-0033, Japan

E-mail: hassy@mat.eng.shizuoka.ac.jp (H Hashimoto)

Received 23 April 2001

Abstract

Terahertz (THz) radiation was generated via optical rectification from organic single crystals, i.e. *N*-substituted (*N*-benzyl, *N*-diphenylmethyl, and *N*-2-naphthylmethyl) derivatives of 2-methyl-4-nitroaniline (MNA), and it was detected by means of the electro-optic sampling method. The intensity and the spectrum of the THz radiation were compared with those of ZnTe and DAST (*N*, *N*-dimethylamino-*N*′-methylstilbazolium p-toluenesulphonate) crystals. The integrated intensity of the THz radiation from the *N*-benzyl-MNA crystal was two thirds of that for the ZnTe crystal, the best-known practical THz emitter, and was as intense as that for the DAST crystal, the best organic THz emitter ever studied. The spectrum of the ZnTe crystal extended to 3 THz, while that of the *N*-benzyl MNA and DAST crystals dropped off around 2.5 THz. The THz radiation intensities from all of the organic crystals were compared quantitatively, on the basis of the consideration of molecular arrangements in the crystals. It was suggested that the absorption due to low-frequency phonon modes affected both the intensity and the spectral band shape of the THz radiation.

Electromagnetic radiation in the far-infrared spectral region attracts much attention these days owing to its potential applications in spectroscopy, imaging, telecommunications, medical analysis, and so on [1]. The radiation is usually called terahertz (THz) radiation in view of its frequency, in between those of light and electric waves. The applications of THz radiation used to be restricted due to the difficulty of generation and detection of this frequency

[4] Author to whom any correspondence should be addressed. Present address: Division of Biochemistry and Molecular Biology, Institute of Biomedical and Life Sciences, Davidson Building, University of Glasgow, Glasgow G12 8QQ, UK.

0953-8984/01/230529+09$30.00

range. However, owing to the development of ultrashort-pulsed laser techniques, now one can readily generate and detect THz radiation if good nonlinear optical crystals having enough macroscopic second-order nonlinearity are available [2]. That is, the pulsed THz radiation can be generated via optical rectification from the nonlinear crystal irradiated with ultrashort (shorter than subpicosecond) laser pulses. The THz pulses thus generated are coherent with the excitation laser pulses. Therefore, they can readily be detected by means of an electro-optic (EO) sampling method. Since the subpicosecond optical rectification used in this study can accurately be considered as the difference-frequency mixing [3], nonlinear optical coefficients (d-constants) of the crystals are relevant to the yield of the THz generation (see below). On the other hand, the EO sampling method solely depends on the electro-optic properties of the nonlinear crystals [4]; hence the electro-optic coefficients (r-constants) of the crystals are related to the detection sensitivity of the THz radiation.

Nonlinear optical crystals with enough second-order macroscopic nonlinearity are necessary in order to generate the THz radiation effectively using the lower-intensity subpicosecond laser pulses. The THz radiation thus generated from inorganic crystals such as $LiTaO_3$, GaAs, and ZnTe, as well as from organic crystals such as 2-methyl-4-nitroaniline (MNA) and N, N-dimethylamino-N'-methylstilbazolium p-toluenesulphonate (DAST), has already been reported [2]. In an earlier paper, we reported the preliminary characteristics of the THz radiation from N-benzyl-MNA and DAST emitters, and discussed the effect of laser damage on the crystals [5]. It is generally accepted that inorganic nonlinear crystals are the superior choice in terms of durability against intense laser light irradiation. However, development of organic nonlinear crystals is increasingly desired owing to their higher nonlinearity as well as promising applications in an all-plastic THz generation system. In fact, the organic crystals can sometimes be a better choice when frequency dispersion is taken into consideration [6]. As regards the development of organic nonlinear crystals, we succeeded in improving both the macroscopic second-order nonlinearity and the crystal habit of MNA by introducing benzyl-type substituent groups [7]. Further, we were able to explain successfully the second-harmonic (SH) intensities of the crystals quantitatively by taking the molecular arrangements in the crystals into consideration [8]. In this study, we have compared the THz radiation characteristics of some N-substituted MNA crystals. The main objective of the present research is to clarify whether the analysis used to interpret the SH intensities of the MNA crystals is also applicable for explaining the integrated intensities of the THz radiation or not. The spectral band shape of the THz radiation is also discussed, taking the low-frequency phonon modes into account.

Figure 1 shows the chemical structures of the organic molecules used in this study. The single crystals grown from all of the molecules shown in figure 1 have macroscopic second-order nonlinearity; the crystals lack a centre of symmetry (see below). The synthesis and x-ray crystallography for the MNA derivatives were described previously [7]. DAST was synthesized by ourselves according to the method described in the literature [9, 10]. The single crystals of these molecules were grown by the solution method [7, 8]. Vibrational analysis for the low-frequency phonon modes as well as frequency-dependent first-order hyperpolarizabilities for optical rectification ($\beta(0; \omega, -\omega)$ tensor components) of the molecules were computed semi-empirically using the MOPAC2000 and MOS-F 4.2 software packages (Fujitsu), respectively. The initial geometry set for the calculation was carried over from the results of x-ray crystallography. (X-ray crystallography of the DAST crystal at room temperature was carried out by ourselves using a Rigaku AFC-7R diffractometer with graphite-monochromated Cu Kα radiation and a 12 kW rotating-anode generator.) Geometry optimization and vibrational analysis were performed using an AM1 Hamiltonian. The thus-optimized structure of each molecule did not deviate very much from that determined by x-ray crystallography.

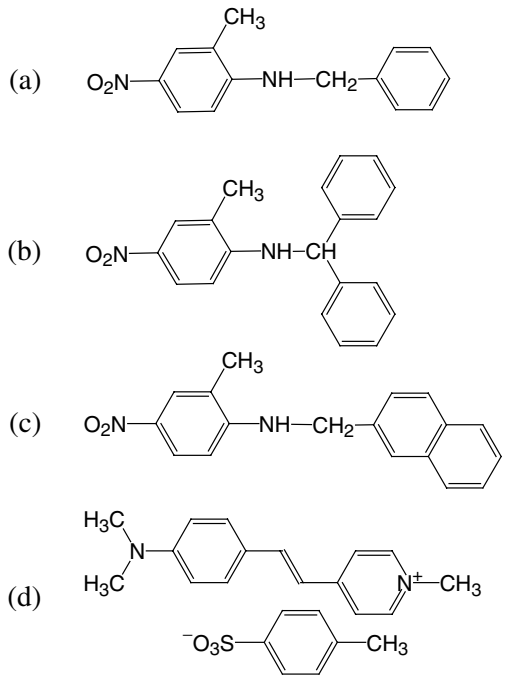

Figure 1. Chemical structures of (a) *N*-benzyl-2-methyl-4-nitroaniline (*N*-benzyl-MNA), (b) *N*-diphenylmethyl-2-methyl-4-nitroaniline (*N*-diphenylmethyl-MNA), (c) *N*-2-naphthylmethyl-2-methyl-4-nitroaniline (*N*-2-naphthylmethyl-MNA), and (d) *N*, *N*-dimethylamino-*N*′-methyl-stilbazolium p-toluenesulphonate (DAST).

The $\beta(0; \omega, -\omega)$ components were computed by means of an INDO-CI method using the optimized structures.

Figure 2 is a schematic illustration of our experimental set-up. A mode-locked Ti:sapphire laser (Spectra-Physics Tsunami) with a pulse duration of 100 fs at a wavelength of 800 nm was used as the optical pulse source. The laser beam was split into pump and probe pulses with a beam splitter. The pump pulse is intermittently blocked with an optical chopper at a 4.2 kHz rate. The pulse was focused on the (110) plane of ZnTe, the (100) plane of *N*-benzyl-MNA, and the (001) plane of the *N*-diphenylmethyl-MNA, *N*-2-naphthylmethyl-MNA, and DAST emitter crystals at a normal-incidence angle using a $\times 10$ objective lens. Each crystal was set on the silicon (Si) spherical lens using Si grease. The pump power at the emitter was 40 mW. The free-space THz beam generated from the emitter was reflected using the off-axis paraboloidal mirrors through Si lenses and it was detected by the EO sampling method using a 65 μm thick ZnTe(110) crystal. The temporal waveforms were acquired by varying the time delay of the probe light. Since we could only detect the THz beam with horizontal polarization, the emitter crystals were rotated in the (001) plane to get the largest THz signals. The fast-Fourier-transform (FFT) amplitude spectra of the THz output signals were calculated from the temporal waveforms.

Figure 3 shows the temporal waveform (left-hand side) and FFT amplitude spectra (right-hand side) of (a) ZnTe, (b) *N*-benzyl-MNA, (c) *N*-2-naphthylmethyl-MNA, and (d) DAST crystals. The THz radiation from *N*-diphenylmethyl-MNA crystal was too weak to be detected. All of the results in figure 3 can be quantitatively compared with each other. In the previous preliminary report of results on ZnTe, *N*-benzyl-MNA, and DAST crystals, some small dips

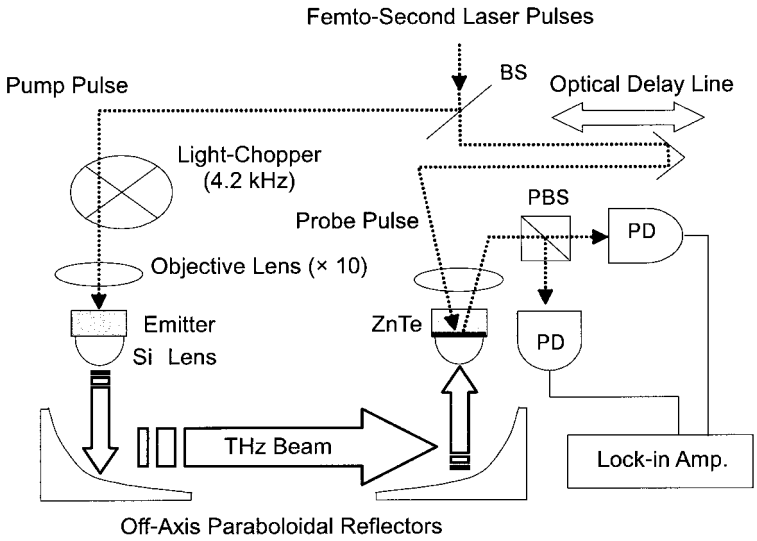

Figure 2. The experimental set-up for subpicosecond optical rectification and electro-optic sampling. BS, PBS, and PD denote, respectively, the beam splitter, polarized beam splitter, and photo-diode.

appeared in the FFT amplitude spectrum, caused by the reflection of the THz waves at the interfaces of the Si lens [5]. In this study, we have eliminated this effect by filtering the FFT amplitude spectra, assuming damped oscillators. The dip observed at 1.8 THz common to figures 3(a), 3(b), and 3(c) is due to absorption by water vapour. The DAST crystal shows additional absorption due to intra-molecular phonons in the 0.9 to 1.2 THz region (see below). We could barely detect the THz radiation from the *N*-2-naphthylmethyl-MNA crystal, but electronic noise in the detector system causes substantial deterioration of the temporal waveform of the signal. The sharp peaks at 0.4 and 0.9 THz in its FFT amplitude spectrum are attributed to the noise.

Table 1 summarizes (1) integrated THz intensities relative to that of ZnTe crystal, (2) the SH intensities relative to that of urea determined by a powder method [7], and (3) space group symmetries of the present organic crystals. Both *N*-benzyl-MNA and DAST crystals can emit THz radiation with two thirds of the intensity of that from the ZnTe crystal. On the

Table 1. Physical and optical properties of the crystals of MNA derivatives and DAST and semi-empirically computed averaged molecular hyperpolarizabilities $||\beta||$ (10^{-30} cm^5/esu) and the **b**-tensor components, where X, Y, and Z denote the crystal axes (10^{-30} cm^5/esu). 'I' is intensity.

Compound	THz intensity ($\times I_{\mathrm{ZnTe}}$)	SH intensity ($\times I_{\mathrm{urea}}$)	Symmetry group	$\|\|\beta\|\|$	$\|b_{XXX}\|$	$\|b_{XZZ}\|$	$\|b_{ZXX}\|$	$\|b_{ZYY}\|$	$\|b_{ZZZ}\|$	$\|b_{XYZ}\|$
N-benzyl-MNA	0.62	300	$Pna2_1$	16.5			9.25	2.12	13.9	
N-diphenylmethyl -MNA	0	10	$P2_12_12_1$	18.6						4.31
N-2-naphthylmethyl -MNA	5.2×10^{-3}	120	$P2_12_12_1$	16.5						6.53
DAST	0.65	1000[a]	Cc	198	6.34	59.3	20.8		155	

[a] From references [9, 10].

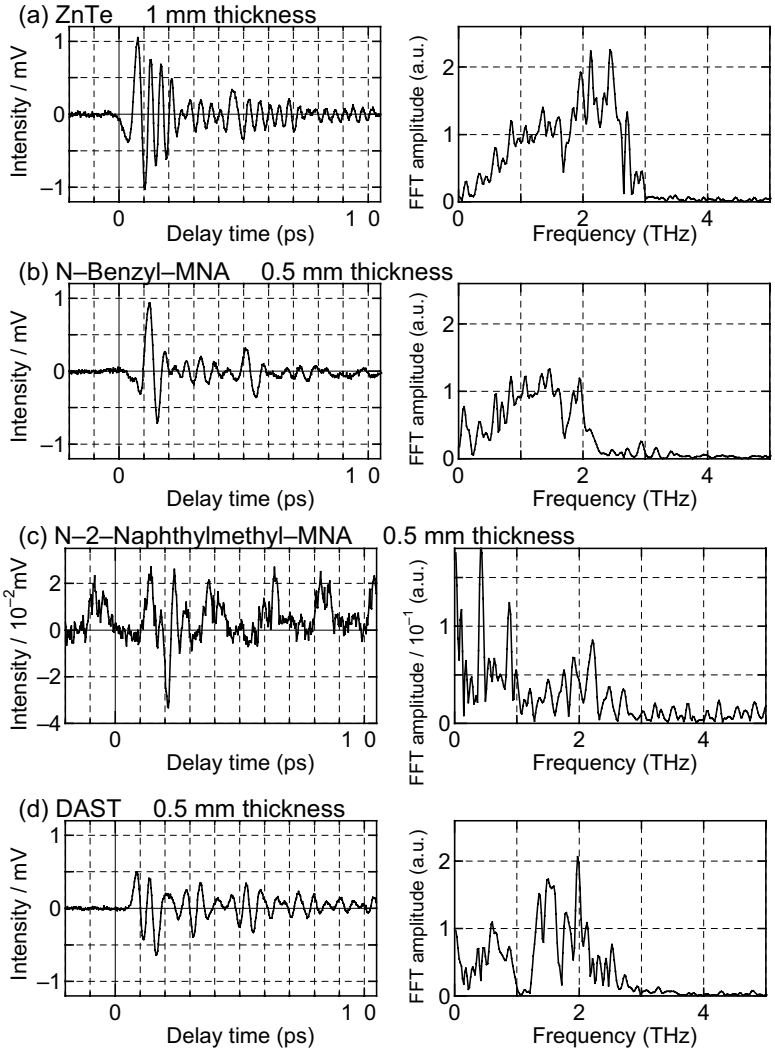

Figure 3. Temporal waveforms (left) and FFT amplitude spectra (right) of the THz radiation from (a) ZnTe(001), (b) *N*-benzyl-MNA(100), (c) *N*-2-naphthylmethyl-MNA(001), and (d) DAST(001) crystals.

other hand, the THz radiation intensity of the *N*-2-naphthylmethyl-MNA crystal is negligibly small; it is as low as 5×10^{-3} times that of ZnTe. The fact that the THz radiation from the *N*-diphenylmethyl-MNA crystal was not detected can be accounted for on the basis of a comparison of its SH intensity (10 times that of urea), which is an order of magnitude smaller than that of *N*-2-naphthylmethyl-MNA which belongs to the same $P2_12_12_1$ space group. The most striking finding in this investigation is that the THz intensity from *N*-benzyl-MNA is as intense as that of DAST, although the SH intensity of DAST (1000 times that of urea) is more than three times larger than that of *N*-benzyl-MNA (300 times that of urea). The very weak THz intensity from *N*-2-naphthylmethyl-MNA is also not accounted for on the basis of the SH intensity (120 times that of urea). It would be intriguing to investigate this discrepancy on the basis of the molecular arrangements in these crystals.

In the previous analysis based on the oriented gas model, we reported that the **b**-tensor, which depends only on the crystal symmetry and shows the unit-cell nonlinearity per molecule in the crystal, can be a good measure in the qualitative comparison of the SH activities of the crystals [7]. Further, we have succeeded in explaining quantitatively the SH intensities on the basis of the calculation of the space-averaged values of the squares of the d-constants derived from the **b**-tensor components [8]. The optical rectification usually relates to the generation of a dc polarization in a nonlinear medium by an intense optical beam [3]. The dc polarization does not radiate but creates an electric field in the medium. However, an intense pulsed light beam induces the subpicosecond optical rectification used in this study. Therefore, the polarization in the medium is time dependent and can radiate electromagnetic waves. For more accurate consideration, subpicosecond optical rectification could be considered as difference-frequency generation [11]. When a pulsed light beam, containing a broad frequency spectrum determined by the shape and duration of the pulse, is incident upon a nonlinear optical sample, the nonlinear interaction between any two frequency components will induce a polarization and radiate electromagnetic waves at their beat frequency. This radiation has a continuous spectrum with a frequency as high as several THz and a special waveform. In the sample, the component of nonlinear dielectric polarization at frequency Ω can be approximately expressed as

$$P_i(\Omega) = \varepsilon_0 \int_{\omega_0-\Delta\omega/2}^{\omega_0+\Delta\omega/2} d_{ijk}(-\Omega;\, \omega+\Omega,\, -\omega) E_j(\omega+\Omega) E_k^*(\omega)\, \mathrm{d}\omega \tag{1}$$

where ω_0 is the central frequency of the incident light beam and $\Delta\omega$ is the bandwidth of the incident light beam with $\Delta\omega \geqslant 1/\tau \approx 10^{12}$ Hz when the incident pulse duration τ is in the subpicosecond range. The frequency Ω ranges from 0 to $\Delta\omega$. $E_j(\Omega+\omega)$ and $E_k^*(\omega)$ are the Fourier transforms of the electrical components of the incident light beam. $d_{ijk}(-\Omega;\, \omega+\Omega,\, -\omega)$ refers to the nonlinear optical coefficients of the crystals. The i-, j-, and k-values run from 1 to 3 and refer to the crystallographic axes of the crystals.

When the central frequency ω_0 for the incident light beam is far from the resonant frequency of the crystals as in the present study, the nonlinear optical coefficients have little frequency dependence, and $d_{ijk}(-\Omega;\, \omega+\Omega,\, -\omega)$ can be considered to be independent of the frequency ω and can be written as d_{ijk}^{Ω}. The nonlinear optical coefficients can be factored out from the above integral, and the integral can be evaluated with the known incident pulsed beam. By the dipole radiation approximation in the far field, the component of the radiated electric field at a certain frequency Ω is proportional to the dipole polarization $P(\Omega)$ and can be written as [12]

$$E^{rd}(\Omega) \approx \Omega^2 P(\Omega) \approx \Omega^2 d_{ijk}^{\Omega} \int_{\omega_0-\Delta\omega/2}^{\omega_0+\Delta\omega/2} E_j(\omega+\Omega) E_k^*(\omega)\, \mathrm{d}\omega. \tag{2}$$

Therefore the THz intensity is proportional to the d-constants that have a close relation with the **b**-tensor components.

There are 27 components in the **b**-tensor. Crystal point group symmetry and Kleinman relations reduce the number of its nonzero components. Three components b_{ZZZ}, b_{ZYY}, and b_{ZXX} remain in the $Pna2_1$ space group, only one component b_{XYZ} remains in the $P2_12_12_1$ space group, and six components b_{XXX}, b_{ZZZ}, b_{XYY}, b_{ZYY}, b_{XZZ}, and b_{ZXX} remain in the Cc space group. According to the geometrical considerations for the molecular arrangements in the crystals, the **b**-tensor components can be explicitly described using the first-order molecular hyperpolarizabilities (β) [13]. We have already reported the expressions for the $Pna2_1$ (N-benzyl-MNA) and $P2_12_12_1$ (N-diphenylmethyl-MNA and N-2-naphthylmethyl-MNA) space groups [7]. For the Cc space group (DAST), the relations can be given as follows:

$$\begin{array}{lll} b_{XXX} = \beta_{xxx} & b_{ZZZ} = -\beta_{yyy}\sin^3\alpha & b_{XYY} = \beta_{yyx}\cos^2\alpha \\ b_{ZYY} = -\beta_{yyy}\cos^2\alpha\sin\alpha & b_{XZZ} = \beta_{xyy}\sin^2\alpha & b_{ZXX} = -\beta_{yxx}\sin\alpha. \end{array} \tag{3}$$

Here X, Y, and Z denote crystal axes, and x, y, and z denote molecular axes. α is an angle determined when the angle between the two equivalent molecular planes is set to $\pi - 2\alpha$. According to the results of x-ray crystallography of DAST, it was clarified that the molecular planes of neighbouring stilbazolium ions (sulphonate ions) were parallel to each other (see for example reference [10]). Therefore, α turns out to be equal to $\pi/2$ in the case of DAST. In this case, the b_{XYY}- and b_{ZYY}-components in equation (3) vanish, and only four components b_{XXX}, b_{ZZZ}, b_{XZZ}, and b_{ZXX} remain nonzero.

Table 1 shows the averaged molecular hyperpolarizabilities $||\beta||$ and the **b**-tensor components of the present organic crystals. The $\beta(0; \omega, -\omega)$ values at 800 nm were predicted on the basis of an INDO-CI molecular orbital calculation that is believed to be very reliable [7]. The $||\beta||$ values of N-benzyl-MNA (16.5) and DAST (198) ascribe a more than three times larger SH intensity to DAST than to N-benzyl-MNA. In the present experimental set-up of subpicosecond optical rectification, we excite the (100) plane of the N-benzyl-MNA crystal normally. Therefore the light wave propagates along the X-direction of the crystal, and the nonlinear polarization is induced in the YZ-plane of the crystal. In consequence, two of the three **b**-tensor components $|b_{ZYY}|$ and $|b_{ZZZ}|$ are relevant to the THz radiation, and the largest component $|b_{ZZZ}|$ should be responsible for the present observation. As regards the DAST crystal irradiated on its (001) plane, the light wave propagates along the Z-direction and the nonlinear polarization is induced in the XY-plane of the crystal. Hence, two of four **b**-tensor components $|b_{XXX}|$ and $|b_{ZXX}|$ are effective as regards the THz radiation. Since nonlinear polarization induced by the component $|b_{ZXX}|$ is along the Z-direction of the crystal, the larger value of the tensor component (20.8) is not directly available for the generation of the THz radiation. This is why THz radiations with similar intensities were detected for N-benzyl-MNA and DAST. The largest **b**-tensor component is found for $|b_{ZZZ}|$ (155) in DAST. This is a good indication that an order-of-magnitude more intense THz radiation than that of the present case is expected on irradiating the crystal from the X- or Y-direction. This finding is quite consistent with the recent observation by Souma *et al* [14]. In the case of N-diphenylmethyl-MNA and N-2-naphthylmethyl-MNA crystals, only one tensor component $|b_{XYZ}|$ can be responsible for the THz generation. However, nonlinear polarization is induced only along the X- or Y-direction when the crystals are irradiated on their (001) plane. Therefore, this particular tensor component is not effective for the present investigation.

Finally, we discuss the spectral dependence of the THz radiation intensity. As shown in figure 3, the FFT amplitude spectrum of ZnTe spreads to 3 THz. On the other hand, the spectral width of N-benzyl-MNA is limited to 2.1 THz and that of DAST spreads over 2.5 THz. According to equation (2), the spectral band shape of the THz radiation should be unique when the d-constants can be considered to be independent of the frequency ω. The marked differences of these spectra are most reasonably attributed to absorption by low-frequency phonons. Figure 4 shows the low-frequency phonon modes predicted by MNDO-AM1 molecular orbital calculations. The result for DAST resembles the far-infrared absorption spectra reported by Walther *et al* [15]; hence we can rely on the results of the present semi-empirical molecular orbital calculations. A strong phonon mode around 2.3 THz is observed for N-benzyl-MNA. In the case of DAST, a number of strong phonon modes appear above 2.5 THz. The presence of these phonon modes is consistent with the cut-off frequency of the THz radiation of these crystals. As regards ZnTe crystal, low-frequency phonons above 3 THz [16] restrict its spectral band shape. We could barely observe the THz radiation from the N-2-naphthylmethyl-MNA crystal, while the THz radiation from the N-diphenylmethyl-MNA crystal was below the detection limit. As shown in figure 4(b), the number of phonon modes of N-diphenylmethyl-MNA is greater than that of N-2-naphthylmethyl-MNA in the 0 to 2.5 THz region. This is another reason for the weak THz radiation.

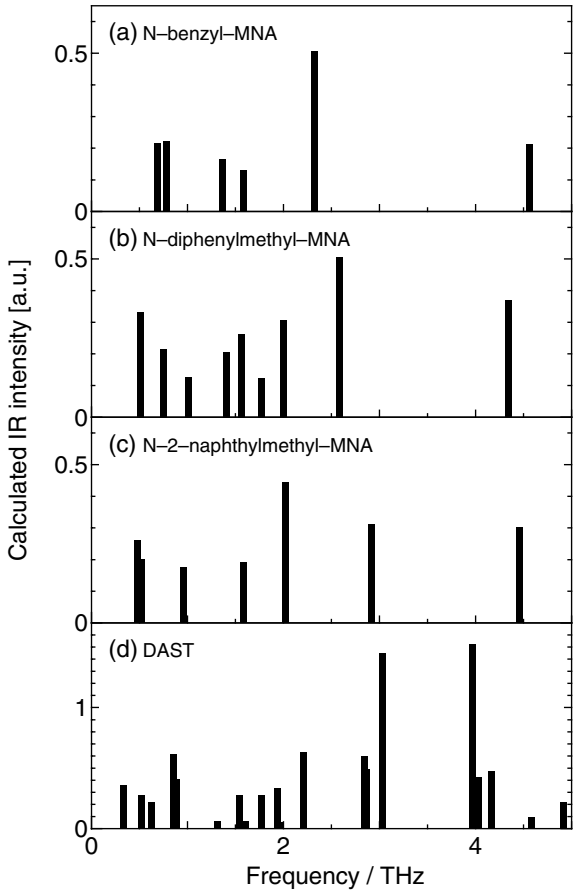

Figure 4. Intensities and frequencies of low-frequency phonon modes evaluated by MNDO-AM1 molecular orbital calculations for (a) *N*-benzyl-MNA, (b) *N*-diphenylmethyl-MNA, (c) *N*-2-naphthylmethyl-MNA, and (d) DAST molecules.

In conclusion, the integrated intensities of the THz radiation from *N*-benzyl-MNA, *N*-diphenylmethyl-MNA, *N*-2-naphthylmethyl-MNA, and DAST crystals were explained well by taking the **b**-tensor components into consideration. Also, the spectral band shape of the THz radiation was examined, taking the absorption due to the low-frequency phonon modes into account.

HH is grateful for the grant-in-aid (grants No 10740145 and No 1240179) from the Ministry of Education, Culture, Sports, Science and Technology. This work was partly supported by Research for the Future of Japan Society for the Promotion of Science (JSPS-RFTF-97P-00101)

References

[1] Mittleman D M, Jacobsen R H, and Nuss M C 1996 *IEEE J. Selected Top. Quantum Electron.* **2** 679
[2] Ma X F and Zhang X C 1993 *J. Opt. Soc. Am.* B **10** 1175
[3] Bass M, Franken P A, Ward J F and Weinreich G 1962 *Phys. Rev. Lett.* **9** 446
[4] Zhang X C, Jin Y and Ma X F 1992 *Appl. Phys. Lett.* **61** 2764

[5] Takahashi H, Hosoda M, Aoshima S, Yamada T and Hashimoto H 1999 *Proc. 7th IEEE Int. Conf. on Terahertz Electronics* (New York: IEEE) p 129
[6] Han P Y, Tani M, Pan F and Zhang X C 2000 *Opt. Lett.* **25** 675
[7] Hashimoto H, Okada Y, Fujimura H, Morioka M, Sugihara O, Okamoto N and Matsushima R 1997 *Japan. J. Appl. Phys.* **36** 6754
[8] Hashimoto H, Okada Y, Okamoto N and Matsushima R 2000 *J. Lumin.* **87–89** 886
[9] Marder S R, Perry J W and Shaefer W P 1989 *Science* **245** 626
[10] Marder S R, Perry J W and Yakymyshyn C P 1994 *Chem. Mater.* **6** 1137
[11] Shen Y R 1990 *Principles of Nonlinear Optics* (New York: Wiley) ch 8, p 113
[12] Jackson J D 1975 *Classical Electrodynamics* (New York: Wiley) ch 11, p 395
[13] Zyss J and Oudar J L 1982 *Phys. Rev.* A **26** 2028
[14] Souma S, Kegasawa K, Taniuchi T, Sato T and Ito H 1998 *IEICE Technical Report* LQE98-9, p 49
[15] Walther M, Jensby K, Keiding S R, Takahashi H and Ito H 2000 *Opt. Lett.* **25** 911
[16] Gallot G, Zhang J, McGowan R W, Jeon T I and Grischkowsky D 1999 *Appl. Phys. Lett.* **74** 3450